Direct Imaging of Individual Intrinsic Hydration Layers on Lipid Bilayers at Ångstrom Resolution

Takeshi Fukuma, Michael J. Higgins, and Suzanne P. Jarvis
Centre for Research on Adaptive Nanostructures and Nanodevices, Trinity College Dublin, Dublin 2, Ireland

ABSTRACT The interactions between water and biological molecules have the potential to influence the structure, dynamics, and function of biological systems, hence the importance of revealing the nature of these interactions in relation to the local biochemical environment. We have investigated the structuring of water at the interface of supported dipalmitoylphosphatidylcholine bilayers in the gel phase in phosphate buffer solution using frequency modulation atomic force microscopy (FM-AFM). We present experimental results supporting the existence of intrinsic (i.e., surface-induced) hydration layers adjacent to the bilayer. The force versus distance curves measured between the bilayer and the AFM tip show oscillatory force profiles with a peak spacing of 0.28 nm, indicative of the existence of up to two hydration layers next to the membrane surface. These oscillatory force profiles reveal the molecular-scale origin of the hydration force that has been observed between two apposing lipid bilayers. Furthermore, FM-AFM imaging at the water/lipid interface visualizes individual hydration layers in three dimensions, with molecular-scale corrugations corresponding to the lipid headgroups. The results demonstrate that the intrinsic hydration layers are stable enough to present multiple energy barriers to approaching nanoscale objects, such as proteins and solvated ions, and are expected to affect membrane permeability and transport.

INTRODUCTION

Water molecules adjacent to biological membranes could potentially play a key role in many important biological processes, particularly when they form hydration layers in which the water molecules are partially ordered due to the interaction with the membrane through dipole potential or hydrogen bonding. If such hydration layers exist, they should alter the local interaction potential at the water/lipid interface, which will significantly influence the function of membrane proteins and molecular transport across the membranes. Membrane hydration is doubly important in biological processes involving membrane-membrane or membrane-vesicle interactions. In these processes, approaching membranes and their constituent molecules should experience the interaction potential presented by the hydration layers of both surfaces, and such interaction can affect the molecular behavior in the subsequent membrane contact or fusion processes. Due to these biologically important issues, the hydration of membrane surfaces has been intensively studied, typically using model lipid bilayers in aqueous environments (1–4).

The short-range (<1 nm) interaction force acting between two apposing lipid bilayers has been measured using the osmotic stress method (5–7) and surface force apparatus (SFA) (8). The measured force versus distance curves showed exponential distance dependence, with a decay length of 0.1–0.3 nm (5–8). Due to the similarity of the decay length to the molecular size of water (9), the short-range force has been attributed to the force required to remove the ordered water molecules in the hydration layers (''hydration force'') (10). However, it has also been claimed that such hydration layers cannot exist due to the disruptive effect of thermally induced molecular-scale protrusions of lipid headgroups and that, alternatively, the repulsive force arising from the overlap of such protrusions (''steric protrusion force'') dominates the short-range force (11,12). Note that the terms ''hydration force'' and ''steric protrusion force'' in this work are used only for referring to the forces specifically defined in this paragraph to avoid confusion. After a number of theoretical and experimental studies supporting one or the other model (13–18), McIntosh and Simon presented another possible model based on a series of force measurements using the osmotic stress method (2). According to their model, the hydration force dominates the short-range force when the separation of the bilayers is >0.4 nm, whereas the steric protrusion force becomes predominant at a closer separation.

Recent progress in various spectroscopic and microscopic techniques has enabled detailed investigations of the ordering of water molecules at water/lipid interfaces (19–25). Since most of the results obtained by those techniques have suggested the ordering of water molecules confined between lipid bilayers, the model presented by McIntosh and Simon has become more and more widely accepted. However, to the best of our knowledge there is a lack of clear experimental evidence to support key features of the model.

For example, there has been no direct experimental evidence for the existence of the steric protrusion force. McIntosh and Simon found that the short-range force at a separation <0.4 nm shows a dependence on the phase of the lipid bilayer (e.g., subgel, gel, and liquid crystalline phases) and hence attributed it to the steric protrusion force (2). However, it has not been clear whether the force arises from the thermal protrusions or simply from the contact of the static bilayers. In the osmotic stress method, the separation of the

Submitted November 8, 2006, and accepted for publication February 5, 2007.
Address reprint requests to Takeshi Fukuma, E-mail: takeshi.fukuma@tcd.ie.

0006-3495/07/05/3603/07 $2.00
doi: 10.1529/biophysj.106.100651

multilamellar bilayers is estimated from the electron density profile obtained from x-ray diffraction data. Thus, the estimated interbilayer distance is averaged over the micrometer-scale area of a number of multilamellar bilayers. Even slight undulations of the surface, or variation in the gap distance, between different pairs of apposing bilayers can produce a gradual increase in the repulsive force with decreasing separation of otherwise ''static'' lipid bilayers.

In addition, there has been no direct experimental evidence for the existence of intrinsic (i.e., surface induced) hydration layers. Most of the experiments that have supported the ordering of water molecules were carried out with multilamellar lipid bilayers where water molecules are confined in a small gap between micrometer-scale membrane surfaces (19–25). Thus, it has been unclear whether the observed ordering is induced by geometrical confinement or interactions with the membrane surface. In addition, most of the existing spectroscopic and microscopic methods provide the ordering or positions of water molecules statistically averaged over micrometer-scale surface area of, in most cases, many multilamellar lipid bilayers (19–25). Therefore, it has not been established whether the intrinsic hydration layers can be sufficiently stable to present multiple energy barriers to the approaching nanoscale objects such as proteins and solvated ions.

Atomic force microscopy (AFM) (26) has a unique capability of measuring local interaction potential with a nanometer-scale cross section using a sharp tip as a force probe. In particular, frequency modulation AFM (FM-AFM) (27) makes it possible to measure quantitative force profiles even within the short-range attractive interaction regime that has not been accessible with static-mode AFM. This capability is potentially very useful to directly probe the interaction forces that nanoscale objects (e.g., proteins and solvated ions) would experience when they approach a membrane surface. To explore this possibility, we have so far presented measurements of force profiles on hydrophilic surfaces such as self-assembled monolayers (28,29) and lipid bilayers (30) in pure water using a carbon nanotube probe. The results showed oscillatory force profiles corresponding to the sequential removal of the ordered water layers between the tip and sample.

Although these results revealed that the approaching nanoscale objects will experience multiple energy barriers next to the lipid membranes, this does not necessarily means that the measured oscillatory force profiles originate from the intrinsic hydration layers. Even with a carbon nanotube probe, the diameter of the probe (10–50 nm) is much larger than the diameter of a water molecule (0.2–0.3 nm) so that geometrical confinement may induce the water molecules to form ordered water layers between the tip and sample. In fact, the force versus distance curves measured on a lipid bilayer in those experiments showed up to five oscillatory peaks (30), which is much more than the number of intrinsic hydration layers expected from molecular dynamics simulations (4). To measure the interaction potential created by the intrinsic hydration layers without geometrical confinement, it is essential to have a sharp tip with a cross section comparable or smaller than the size of water molecules.

In this article, we address these issues based on experimental results obtained by ultra-low noise FM-AFM (31). We present experimental results supporting the existence of intrinsic hydration layers and resultant multiple energy barriers adjacent to a supported dipalmitoylphosphatidylcholine (DPPC) lipid bilayer in the gel phase in phosphate buffer solution. The oscillatory force profiles measured on the membrane surface are presented and discussed in relation to the previously reported nonoscillatory hydration force (2,5–8). The intrinsic hydration layers are visualized by FM-AFM at Ångstrom resolution in real space.

MATERIALS AND METHODS

Sample preparation

The phosphate buffer solution was prepared by dissolving a tablet of phosphate buffer saline (Sigma-Aldrich Ireland, Dublin, Ireland) into 200 ml of pure water. The DPPC bilayer on mica was formed by the vesicle fusion method. DPPC in powder form was dissolved into a mixture of chloroform and methanol (all from Sigma-Aldrich Ireland) to the concentration of 1 mg/ml with a volume content ratio of 3:1. The solution (2–3 ml) was dried in a N_2 gas flow in a glass test tube. Phosphate buffer solution was added to the test tube to the concentration of 0.5 mg/ml and the test tube was ultrasonicated for 5 h at 60°C. After cooling down to room temperature, 45 μl of the DPPC solution and 135 μl of the buffer solution were deposited onto a freshly cleaved mica substrate (round disc with a diameter of 15 mm which was purchased from SPI Supplies, West Chester, PA). The sample was incubated for 30 min at 60°C and rinsed with buffer solution. The DPPC bilayer used in this experiment covers the whole mica surface without any large-scale (>10 nm) defects. We have confirmed that the film is a single bilayer by pushing a tip through the membrane and measuring the film thickness (~4.5 nm) from the force curve using the same method reported in Garcia-Manyes et al. (32).

FM-AFM imaging

In FM-AFM, a microfabricated cantilever with a sharp tip at its end is used for detecting the interaction force acting between the tip and sample. The cantilever is mechanically oscillated at its resonance frequency with constant amplitude (0.29 nm in this experiment) using a self-oscillation circuit. The tip-sample interaction force is detected by measuring the force-induced resonance frequency shift (Δf). For force versus distance curve measurements, Δf values are recorded as a function of tip-sample separation by changing the average vertical tip position at a constant speed. The obtained Δf versus distance curve is converted to a force versus distance curve using the formula reported in Sader and Jarvis (33). The accuracy and validity of the formula have been verified by both theory and experiment (34–36) and the formula is widely used (29,37–41). In FM-AFM imaging, the average vertical tip position is controlled by a feedback circuit such that Δf is kept constant at a preset value referred to as the ''setpoint''. In this way, the average tip-sample distance is effectively kept constant. With this distance regulation feedback, the tip is raster scanned over the sample surface. Since the tip traces the height corrugation of the surface during the scanning, a topographic image is obtained as a two-dimensional map of the control signal for the vertical tip position.

In this experiment, a home-built ultra-low noise FM-AFM (31) is used. The detailed design and performance of the constituent instruments have been described elsewhere (31,42). The FM-AFM has been previously demonstrated to have true atomic resolution (~0.3 nm in xy and 0.01 nm in z) in liquid

(43). The FM-AFM experiments described here were performed at room temperature (21°C) in phosphate buffer solution. The oscillation amplitude of the cantilever was set to 0.29 nm throughout the experiment. Such an extremely small oscillation amplitude has recently been proven to enhance the sensitivity to the short-range interaction force (44) and thereby improve the spatial resolution in vacuum (45,46) and liquid (42,47). The Δf values during the FM-AFM imaging were kept within the range of ± 20 Hz (including fluctuations caused by noise). According to the force versus distance curves obtained in this experiment (shown later), this Δf range approximately corresponds to 0–20-pN load forces. A silicon cantilever (NCH: Nanosensors, Neuchatel, Switzerland) with a spring constant of 34 N/m and a resonance frequency of 134 kHz in buffer solution was used. The spring constant was calibrated by the method reported in Hutter and Bechhoefer (48).

RESULTS

Force versus distance curve measurements

Fig. 1 *A* shows an example of a Δf versus distance curve measured on the DPPC bilayer in phosphate buffer solution. The raw data (*shaded line*) was smoothed (*solid line*) and converted to a force versus distance curve (Fig. 1 *B*). In this way, we obtained 61 force curves at almost the same tip position except for nanometer-scale lateral tip drift (~0.02 nm/s) during the force measurements (3–5 s/curve). In the force measurements, the force curve obtained during the tip approach shows approximately the same profile as that obtained during the tip retraction and hence the vertical tip drift is negligible during force curve acquisition. Among the 61 curves, 19 curves (31%) showed oscillatory profiles with two peaks (Fig. 1 *B*), 31 curves (51%) showed oscillatory profiles with one peak (Fig. 1 *C*), and 11 curves (18%) did not show any oscillatory profile (Fig. 1 *D*). We statistically analyzed the distance between the two peaks in the 19 Δf versus distance curves and obtained a mean distance and standard deviation of 0.28 nm and 0.05 nm, respectively. We carried out force measurements with three different cantilevers of the same type and obtained similar oscillatory force profiles. Thus, the force profiles shown here are not specific to either this particular tip or the location where the force curves were measured. Due to the similarity of the peak distance (0.28 ± 0.05 nm) to the size of a water molecule (9) and reproducibility of the oscillatory force profiles, we conclude that the oscillatory force profile corresponds to the sequential removal of ordered water molecules.

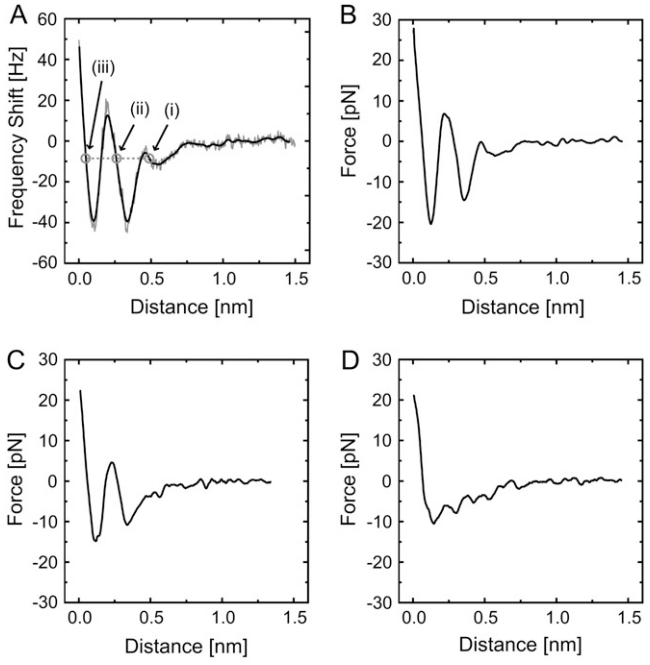

FIGURE 1 (*A*) Example of Δf versus distance curve measured on a DPPC bilayer in phosphate buffer solution, showing an oscillatory profile with two peaks. The smoothed line (*solid*) is obtained by averaging the raw data (*shaded*) over the distance range of ± 0.02 nm from each data point. (*B*) Force versus distance curve converted from (*A*) using the formula reported in Sader and Jarvis (33). (*C*) An example of a force versus distance curve showing an oscillatory profile with one peak. (*D*) An example of a force versus distance curve without any oscillatory profile. The tip velocity during the force curve measurements was 0.5 nm/s. The curves shown here were measured during tip approach. The curves taken during tip retraction show approximately the same profile but were omitted from the figure for clarity.

Three-dimensional characterization

Repulsive and attractive tip-sample interaction forces, respectively, induce positive and negative Δf in FM-AFM. As a tip approaches sample surface, Δf shows steep increase due to the short-range repulsive interaction potential near the surface. Thus, the tip-sample distance feedback regulation in our FM-AFM setup operates based on the assumption that Δf increases with decreasing tip-sample separation such as in the force branches indicated by the arrows *i–iii* in Fig. 1 *A*. Therefore, if the Δf versus distance curve shows an oscillatory profile as shown in Fig. 1 *A*, the feedback can operate at multiple tip positions corresponding to one setpoint, as indicated by the circles in Fig. 1 *A*. These equivalent positions will only be stable provided that the tip does not pass into a region where Δf decreases with decreasing separation. If it does, it will move continuously until it reaches the next equivalent position, such as from *i* to *ii* in Fig. 1 *A*. Thus, the tip can spontaneously jump between those positions even if the setpoint is unchanged.

Fig. 2 shows an example of such spontaneous jumps during FM-AFM imaging of the DPPC bilayer in phosphate buffer solution. In the image shown in Fig. 2 *A*, the tip is scanned from the lowest terrace (Terrace 1). As imaging progresses the tip jumps spontaneously twice. Terrace 1 shows a highly ordered arrangement of bright spots separated by 0.50 ± 0.05 nm along the stripes. A higher magnification image of the same structure is shown in Fig. 2 *D*, which reveals that each bright spot consists of two protrusions separated by 0.30 ± 0.04 nm as indicated by the yellow circle. The first jump of 0.26 nm (Terrace 1–2) results in subtle changes to the image although discrete corrugations are still observed. The second jump of 0.23 nm (Terrace 2–3) results in a less-ordered contrast although imaging resolution is still high.

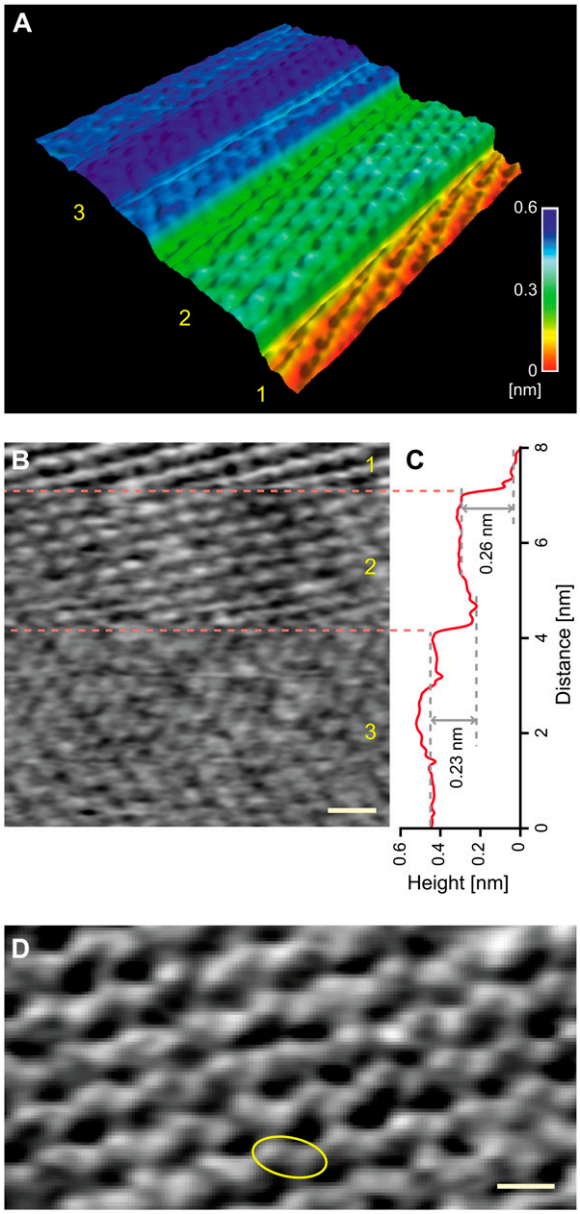

FIGURE 2 (*A*) Example of an FM-AFM image of the DPPC bilayer in phosphate buffer solution showing spontaneous jumps during imaging. Image size: 8 × 8 nm^2. Tip velocity, 120 nm/s. Imaging speed: 85 s/frame. (*B*) Line-by-line flattened image of (*A*). Scale bar, 1 nm. Height range: 0.1 nm (*black* to *white*). Fast and slow scan directions: left to right and top to bottom. The regions indicated by the numbers 1, 2, and 3 correspond to the Terraces 1, 2, and 3 in *A*. (*C*) Line-averaged height profile of (*B*) plotted along the slow scan direction. (*D*) FM-AFM image of the same structure as seen on Terrace 1 in (*A*). Scale bar, 0.5 nm. Height range: 0.12 nm (*black* to *white*). Tip velocity, 146 nm/s. Imaging speed: 7.3 s/frame. Fast and slow scan directions: left to right and top to bottom.

In this experiment, we found 23 spontaneous jumps in 10 images. Among them, 20 jumps (87%) are between Terraces 1 and 2, 2 jumps (9%) are between Terraces 2 and 3, and 1 jump (4%) is between Terraces 1 and 3. We statistically analyzed the height of the 20 jumps between Terraces 1 and 2 and obtained a mean height and standard deviation of 0.29 nm and 0.06 nm, respectively.

Due to the small distance (0.30 ± 0.04 nm) between the two observed protrusions and their well-ordered arrangement, we attribute them to the choline and phosphate subgroups that make up the headgroup. The heights of the spontaneous jumps (0.29 ± 0.06 nm) agree well with the size of a water molecule (9) and the peak distance of the oscillatory force profile (0.28 ± 0.05 nm). This confirms that the tip is jumping between water layers and the individual layers are imaged with molecular-scale corrugations of the lipid headgroups. Although we have assumed that the observed spontaneous jumps are due to the transitions between the force branches shown in Fig. 1 *A*, it is also possible to explain these jumps as transitions between the different force profiles shown in Fig. 1, *B–D*. In that case, the observed jumps should represent the formation of the first and second hydration layers. This point is discussed in more detail below.

DISCUSSION

Tip geometry

To obtain true (i.e., nonaveraged) Ångstrom-scale resolution in FM-AFM, the short-range (<1 nm) interaction force between the tip front atom and the subnanometer-scale surface structure must predominantly influence Δf (49,50). For such a situation to be realized, the tip end must have a nanoscale protrusion having an atomically sharp asperity (51,52). The images in Fig. 2, *B* and *D*, show nonperiodic Ångstrom-scale features as well as well-ordered structures. For example, the angle of the headgroups in Fig. 2 *D* is not perfectly uniform but has some variations. Thus, the subnanometer-scale features resolved in Fig. 2, *B* and *D*, represent nonaveraged, real-space surface structures. If we define the lateral resolution as the minimum distance between two peaks resolved in the image, the lateral resolution for Fig. 2, *B* and *D*, is 0.35 nm and 0.20 nm, respectively. Such lateral resolution, comparable to a single atomic diameter, strongly suggests that the tip has an atomically sharp asperity.

We obtained true Ångstrom-level resolution both before and after measuring the force curves shown in Fig. 1. For example, Fig. 2, *A* and *D*, is obtained before and after the measurement of Fig. 1 *A*, respectively. Thus, the oscillatory force profiles shown in Fig. 1 represent the short-range interaction force between an atomically sharp tip and the bilayer surface. In addition, the oscillatory force profiles shown in Fig. 1, *B* and *C*, are nearly symmetrical with respect to zero force, which strongly suggests that the mesoscopic-scale tip geometry is also sharp and that the long-range interaction force acting on the mesoscopic-scale tip is negligible compared to the short-range force acting on the nanoscale protrusion at the end of the tip, at least in this distance regime. This is also supported by the magnitude of the oscillatory force (20–30 pN) measured in this experiment, which is much

smaller than those observed in the previous studies using relatively blunt tips, where 200–1000-pN oscillatory forces were measured superimposed on a large background repulsive force (28–30).

Intrinsic hydration layers

There is substantial evidence to suggest that the observed oscillatory force profiles originate from the ordering of the water molecules between the tip and the lipid headgroups. However, the origin for the ordering of water molecules requires further discussion. There are three possible origins: geometrical confinement, tip hydration, and membrane hydration. Due to the atomically sharp tip asperity, it is unlikely that geometrical confinement between the tip and the lipid headgroups can induce water molecules to form stable hydration layers. Thus the ordering must be due to the hydration of either tip or membrane surface. It is very difficult to experimentally determine if the water molecules are associated with the tip or lipid headgroups. However, we have some reasons to believe that it is more likely to be membrane hydration.

First of all, the characteristic oscillatory force profile does not show significant difference for three different tips that were used in our experiments, which suggests that the ordering of the water molecules is relatively insensitive to the atomic-scale tip geometry. Second, the force measurements and imaging show that there are up to two hydration layers in the case of a DPPC bilayer, which is consistent with the molecular dynamics simulations suggesting the existence of 2–3 intrinsic hydration layers next to a lipid bilayer (4,53,54). In particular, the calculated density profile of water molecules next to a DPPC bilayer recently reported by Berkowitz et al. shows remarkable resemblance to the force profile obtained in this experiment (Fig. 1 *B*) (4). Such a good agreement with theory supports the notion that the water layers observed in our experiments are intrinsic hydration layers next to the lipid membrane.

Dynamics of hydration layers

We observed variations in the oscillatory force profiles as shown in Fig. 1, *B–D*. Since these variations are observed even in successive force curves, measured at almost the same tip position, these variations would appear to be time dependent rather than site dependent. Note that the effect of lateral drift of the tip ($\sim$0.02 nm/s) during the force measurements (3–5 s/curve) is hardly an issue because of the nanometer-scale lateral extent of the force profile demonstrated in Fig. 2 *A*. The tip-induced perturbation is unlikely to be responsible for the variation because of the good agreement of the force profiles obtained during the tip approach and retraction processes. Therefore, we conclude that the observed variation corresponds to the time-dependent changes of the number of hydration layers at the local area.

The statistical analysis of the obtained force curves implies that there is one hydration layer for most of the time (Fig. 1 *C*, 50%) while it sometimes disappears (Fig. 1 *D*, 20%) and sometimes another layer appears on top of it (Fig. 1 *B*, 30%). Although Fig. 1 *D* shows no oscillatory peak, the curve shows relatively large fluctuations over the distance range (0.2–0.6 nm) in the region where other curves (Fig. 1, *B* and *C*) show clear oscillations. This indicates that there may be some water molecules associated with the surface but that they are not stable enough to present a clear energy barrier at that moment.

If the spontaneous jumps observed in Fig. 2 *A* correspond to the transitions between the force branches shown in Fig. 1 *A*, this force profile must persist for the whole image acquisition time of 85 s for the imaging to remain stable. Even if they represent the transitions between the different force profiles shown in Fig. 1, *B–D*, each force profile must persist at least for the time required to image the individual terraces in Fig. 2 *A* ($>$10 s). Thus, the formation and disappearance of the hydration layers take place on a relatively slow timescale (several seconds).

Although we have attributed the oscillatory force profile to multiple energy barriers presented by hydration layers, we do not suggest or dispute the possible existence of solid ice-like static layers of water molecules at the water/lipid interface based on these data. The timescale of the AFM measurement is of the order of seconds so that the influence from all molecular diffusion faster than that timescale is averaged. What we can measure with AFM is resultant interaction potential reflecting the statistical average of the positions of water molecules and dipole potential induced by the water molecules. However, the stable imaging on each hydration layer strongly suggests that the interlayer diffusion rates are likely to be slow compared to the imaging time whereas lateral diffusion rates could be much faster.

Hydration and steric protrusion forces

In this experiment, we observed oscillatory force profiles next to a single DPPC bilayer, which strongly suggests that a hydration force will exist between apposing bilayers. However, previous studies using SFA and the osmotic stress method showed nonoscillatory force profiles between DPPC bilayers (2,5–8). Since SFA utilizes supported lipid bilayers and shows similar force profiles to those obtained by the osmotic stress method using unsupported bilayers, the nonoscillatory force profiles cannot be explained by the difference between supported and unsupported bilayers. In FM-AFM measurements, the force profile is measured on a nanometer-scale local area, whereas it is averaged over a micrometer-scale area in measurements using SFA or the osmotic stress method. Over such a large area, even a slight height corrugation of the lipid surface will result in a local variation of the surface separation, which may well smear out the short-range oscillatory force profiles due to global averaging. Such global averaging effects have also been suggested by molecular dynamics simulation studies (4,53,54).

Our force measurements reveal that the statistical average of the number of the intrinsic hydration layers is ~1.1, which suggests the existence of 2–3 intrinsic hydration layers between two apposing lipid bilayers. The osmotic stress measurements by McIntosh and Simon have suggested that the hydration force dominates the short-range interaction force if the bilayer separation is 0.4–1.0 nm for lipid bilayers in the gel phase (2), which corresponds to the thickness of 2–3 water layers. This agreement suggests that the ordering of the water molecules responsible for the hydration force is mainly intrinsic and the influence of geometrical confinement is not significant in the case of two apposing lipid bilayers.

In this experiment, the positions of lipid headgroups are stable enough to be imaged with submolecular resolution (Fig. 2 *D*). In addition, Fig. 2 *A* reveals the stable existence of the hydration layers, which are not disrupted by the thermal motion of the headgroups. Although large-scale (>30 nm) FM-AFM images showed ~0.1-nm height corrugations across the membrane surface, we could not find any evidence of thermally induced motion of such corrugations. From these results, we conclude that there are no thermally induced molecular protrusions or resultant disruptive effects on the formation of the hydration layers, at least in the case of supported DPPC bilayers in the gel phase. Note that the results may be different for different headgroups, phases, temperatures, and solution conditions.

Multiple energy barriers

One of the most important functions of biological membranes is permeation and transport of ions and molecules. In these processes, the nanoscale solvated ions or molecules experience the local interaction potential next to the membrane surface when they approach the surface. In our experiments, the interaction potential is locally probed with a nanoscale cross section. Thus, the measured forces (Fig. 1) are representative of the forces that approaching solvated ions or molecules would experience. Fig. 1 clearly shows that the force profile is not a globally averaged nonoscillatory smooth force profile but instead is highly oscillatory. This result clearly demonstrates that the hydration layers are stable enough to present multiple energy barriers to approaching nanoscale objects. If the nanoscale object is larger than the size of a water molecule, there is a finite possibility of additional energy barriers as a result of geometrical confinement and/or intrinsic hydration layers next to the object's own surface (30). The energy barriers observed here should thus be regarded as the minimum number likely to be present for nanoscale objects due to the atomic sharpness of the AFM tip in this case.

CONCLUSIONS

We have investigated the hydration and resultant force profile next to supported DPPC bilayers in the gel phase in phosphate buffer solution using FM-AFM. The measured oscillatory force profiles demonstrate that up to two intrinsic hydration layers typically exist next to the membrane surface. These oscillatory force profiles also imply that the nonoscillatory hydration force measured by SFA and the osmotic stress method originate from the global averaging of local oscillatory force profiles. The stable imaging of the headgroups at submolecular resolution reveals that there are no thermally induced molecular protrusions, at least in the case of supported DPPC bilayers in the gel phase. The stable imaging of individual hydration layers at molecular-scale resolution demonstrates that the intrinsic hydration layers are stable enough to present multiple energy barriers to approaching nanoscale objects such as proteins and solvated ions.

The results shown here have also demonstrated that FM-AFM has a unique capability for sensitive localized force measurements and high-resolution imaging. Most of the important membrane processes take place over a nanometer-scale local area. Even for those that appear to be micrometer-scale processes, such as membrane-membrane interactions, global averaging can easily smear out local information that is crucial for their understanding. Therefore, the real-space local information obtained by FM-AFM should provide new insights into the molecular-scale origins underlying many biological processes.

This work was supported by Science Foundation Ireland Research Grant (01/PI.2/C033) and the Human Frontier Science Program.

REFERENCES

1. Leikin, S., V. A. Parsegian, D. C. Rau, and R. P. Rand. 1993. Hydration forces. *Annu. Rev. Phys. Chem.* 44:369–395.
2. McIntosh, T. J., and S. A. Simon. 1994. Hydration and steric pressures between phospholipid bilayers. *Annu. Rev. Biophys. Biomol. Struct.* 23: 27–51.
3. Milhaud, J. 2004. New insights into water-phospholipid model membrane interactions. *Biochim. Biophys. Acta.* 1663:19–51.
4. Berkowitz, M. L., D. L. Bostick, and S. Pandit. 2006. Aqueous solutions next to phospholipid membrane surfaces: insights from simulations. *Chem. Rev.* 106:1527–1539.
5. LeNeveu, D. M., R. P. Rand, and V. A. Parsegian. 1976. Measurement of forces between lecithin bilayers. *Nature.* 259:601–603.
6. Lis, L. J., M. McAlister, N. Fuller, R. P. Rand, and V. A. Parsegian. 1982. Interactions between neutral phospholipid bilayer membranes. *Biophys. J.* 37:657–665.
7. McIntosh, T. J., and S. A. Simon. 1986. Hydration force and bilayer deformation: a reevaluation. *Biochemistry.* 25:4058–4066.
8. Marra, J., and J. N. Israelachvili. 1985. Direct measurements of forces between phosphatidylcholine and phosphatidylethanolamine bilayers in aqueous electrolyte solutions. *Biochemistry.* 24:4608–4618.
9. Franks, F. 2000. Water: A Matrix of Life, 2nd ed. Royal Society of Chemistry, Cambridge.
10. Marcelja, S., and N. Radic. 1976. Repulsion of interfaces due to boundary water. *Chem. Phys. Lett.* 42:129–130.
11. Israelachvili, J. N., and H. Wennerström. 1990. Hydration or steric forces between amphiphilic surfaces? *Langmuir.* 6:873–876.
12. Israelachvili, J. N., and H. Wennerström. 1992. Entropic forces between amphiphilic surfaces in liquids. *J. Phys. Chem.* 96:520–531.
13. Kornyshev, A. A., and S. Leikin. 1989. Fluctuation theory of hydration forces: the dramatic effects of inhomogeneous boundary conditions. *Phys. Rev. A.* 40:6431–6437.

14. Leikin, S., and A. A. Kornyshev. 1990. Continuum electrostatic interactions between planer lattices of dipoles and possible relevance to the hydration forces. *J. Chem. Phys.* 92:6890–6898.

15. Cevc, G. 1991. Hydration force and the interfacial structure of the polar surface. *J. Chem. Soc. Faraday Trans.* 87:2733–2739.

16. Leikin, S., and A. A. Kornyshev. 1991. Mean-field theory of dehydration transitions. *Phys. Rev. A.* 44:1156–1168.

17. Parsegian, V. A., and R. P. Rand. 1991. On molecular protrusions as the source of hydration force. *Langmuir.* 7:1299–1301.

18. Kirchner, S., and G. Cevc. 1994. Hydration of polar interface. *J. Chem. Soc. Faraday Trans.* 90:1941–1951.

19. König, S., E. Sackmann, D. Richter, R. Zorn, C. Carlile, and T. M. Bayerl. 1994. Molecular dynamics of water in oriented DPPC multilayers studied by quasielastic neutron scattering and deuterium-nuclear magnetic resonance relaxation. *J. Chem. Phys.* 100:3307–3316.

20. Ho, C., S. J. Slater, and C. D. Stubbs. 1995. Hydration and order in lipid bilayers. *Biochemistry.* 34:6188–6195.

21. Hübner, W., and A. Blume. 1998. Interactions at the lipid-water interface. *Chem. Phys. Lipids.* 96:99–123.

22. Binder, H., T. Gutberlet, A. Anikin, and G. Klose. 1998. Hydration of the dienic lipid dioctadecadienoylphosphatidylcholine in the lamella phase—an infrared linear dichroism and x-ray study on headgroup orientation, water ordering, and bilayer dimensions. *Biophys. J.* 74: 1908–1923.

23. Zhou, Z., B. G. Sayer, D. W. Hughes, R. E. Stark, and R. M. Epand. 1999. Studies of phospholipid hydration by high-resolution magnetic angle spinning nuclear magnetic resonance. *Biophys. J.* 76:387–399.

24. Ge, M., and J. H. Freed. 2003. Hydration, structure, and molecular interactions in the headgroup region of dioleoylphosphatidylcholine bilayers: an electron spin resonance study. *Biophys. J.* 85:4023–4040.

25. Cheng, J.-X., S. Pautot, D. A. Weitz, and X. S. Xie. 2003. Ordering of water molecules between phospholipid bilayers visualized by coherent anti-Stokes Raman scattering microscopy. *Proc. Natl. Acad. Sci. USA.* 100:9826–9830.

26. Binnig, G., C. F. Quate, and Ch. Gerber. 1986. Atomic force microscope. *Phys. Rev. Lett.* 56:930–933.

27. Albrecht, T. R., P. Grutter, D. Horne, and D. Rugar. 1991. Frequency modulation detection using high-Q cantilevers force enhanced force microscope sensitivity. *J. Appl. Phys.* 69:668–673.

28. Jarvis, S. P., T. Uchihashi, T. Ishida, H. Tokumoto, and Y. Nakayama. 2000. Local solvation shell measurement in water using a carbon nanotube probe. *J. Phys. Chem. B.* 104:6091–6094.

29. Uchihashi, T., M. J. Higgins, Y. Nakayama, J. E. Sader, and S. P. Jarvis. 2005. Quantitative measurement of solvation shells using frequency modulated atomic force microscopy. *Nanotechnology.* 16:S49–S53.

30. Higgins, M. J., M. Polcik, T. Fukuma, J. E. Sader, Y. Nakayama, and S. P. Jarvis. 2006. Structured water layers adjacent to biological membranes. *Biophys. J.* 91:2532–2542.

31. Fukuma, T., and S. P. Jarvis. 2006. Development of liquid-environment frequency modulation atomic force microscope with low noise deflection sensor for cantilevers of various dimensions. *Rev. Sci. Inst.* 77:043701.

32. Garcia-Manyes, S., G. Oncins, and F. Sanz. 2005. Effect of ion-binding and chemical phospholipid structure on the nanomechanics of lipid bilayers studied by force spectroscopy. *Biophys. J.* 89:1812–1826.

33. Sader, J. E., and S. P. Jarvis. 2004. Accurate formulas for interaction force and energy in frequency modulation atomic force spectroscopy. *Appl. Phys. Lett.* 84:1801–1803.

34. Sader, J. E., and S. P. Jarvis. 2004. Interaction of frequency modulation atomic force microscopy in terms of fractional calculus. *Phys. Rev. B.* 70:012303.

35. Uchihashi, T., M. J. Higgins, S. Yasuda, S. P. Jarvis, S. Akita, Y. Nakayama, and J. E. Sader. 2004. Quantitative force measurements in liquid using frequency modulation atomic force microscopy. *Appl. Phys. Lett.* 85:3575–3577.

36. Sader, J. E., T. Uchihashi, M. J. Higgins, A. Farrell, Y. Nakayama, and S. P. Jarvis. 2005. Quantitative force measurements using frequency modulation atomic force microscopy: theoretical foundations. *Nanotechnology.* 16:S94–S101.

37. Higgins, M. J., Ch. K. Riener, T. Uchihashi, J. E. Sader, R. McKendry, and S. P. Jarvis. 2005. Frequency modulation atomic force microscopy: a dynamic measurement technique for biological systems. *Nanotechnology.* 16:S85–S89.

38. Farrell, A., T. Fukuma, T. Uchihashi, E. R. Kay, G. Bottari, D. A. Leigh, H. Yamada, and S. P. Jarvis. 2005. Conservative and dissipative force imaging of switchable rotaxanes with frequency-modulation atomic force microscopy. *Phys. Rev. B.* 72:125430.

39. Nishi, R., D. Miyagawa, Y. Seino, I. Yi, and S. Morita. 2006. Noncontact atomic force microscopy study of atomic manipulation on an insulator surface by nanoindentation. *Nanotechnology.* 17:S142–S147.

40. Heyde, M., M. Sterrer, H.-P. Rust, and H.-J. Freund. 2006. Frequency modulated atomic force microscopy on MgO(001) thin films: interpretation of atomic image resolution and distance dependence of tip-sample interaction. *Nanotechnology.* 17:S101–S106.

41. Heyde, M., M. Kulawik, H.-P. Rust, and H.-J. Freund. 2006. Frequency-modulated atomic force spectroscopy on NiAl(110) partially covered with a thin alumina film. *Phys. Rev. B.* 73:125320.

42. Fukuma, T., M. Kimura, K. Kobayashi, K. Matsushige, and H. Yamada. 2005. Development of low noise cantilever deflection sensor for multienvironment frequency-modulation atomic force microscopy. *Rev. Sci. Instrum.* 76:053704.

43. Fukuma, T., K. Kobayashi, K. Matsushige, and H. Yamada. 2005. True atomic resolution in liquid by frequency-modulation atomic force microscopy. *Appl. Phys. Lett.* 87:034101.

44. Giessibl, F. J., H. Bielefeldt, S. Hembacher, and J. Mannhart. 1999. Calculation of the optimal imaging parameters for frequency modulation atomic force microscopy. *Appl. Surf. Sci.* 140:352–357.

45. Giessibl, F. J., S. Hembacher, H. Bielefeldt, and J. Mannhart. 2000. Subatomic features on Si(111)-(7×7) surface observed by atomic force microscopy. *Science.* 289:422–425.

46. Giessibl, F. J. 2000. Atomic resolution on Si(111)-(7×7) by noncontact atomic force microscopy with a force sensor based on a quartz tuning fork. *Appl. Phys. Lett.* 76:1470–1472.

47. Fukuma, T., K. Kobayashi, K. Matsushige, and H. Yamada. 2006. True molecular resolution in liquid by frequency-modulation atomic force microscopy. *Appl. Phys. Lett.* 86:193108.

48. Hutter, J. L., and J. Bechhoefer. 1993. Calibration of atomic-force microscope tips. *Rev. Sci. Instrum.* 64:1868–1873.

49. Giessibl, F. J. 2003. Advances in atomic force microscopy. *Rev. Mod. Phys.* 75:949–983.

50. Fukui, K., and Y. Iwasawa. 1999. Observation of a new ridge structure along steps on the MgO (100) surface by non-contact atomic force microscopy. *Surf. Sci.* 441:529–541.

51. Bennewitz, R., A. S. Foster, L. N. Kantorovich, M. Bammerlin, Ch. Loppacher, S. Schär, M. Guggisberg, E. Meyer, and A. L. Shluger. 2000. Atomically-resolved edges and kinks of NaCl islands on Cu(111): experiment and theory. *Phys. Rev. B.* 62:2074–2084.

52. Barth, C., A. S. Foster, M. Reichling, and A. L. Shluger. 2001. Contrast formation in atomic resolution scanning force microscopy on CaF_2: experiment and theory. *J. Phys. Condens. Matter.* 13:2061–2079.

53. Pandit, S. A., D. Bostick, and M. L. Berkowitz. 2003. An algorithm to describe molecular scale rugged surfaces and its application to the study of water/lipid bilayer interface. *J. Chem. Phys.* 119:2199–2205.

54. Bhide, S. Y., and M. L. Berkowitz. 2005. Structure and dynamics of water at the interface with phospholipid bilayers. *J. Chem. Phys.* 123:224702.